Eur Biophys J (2010) 39:689–698
DOI 10.1007/s00249-009-0556-4

ORIGINAL PAPER

Non-native hydrophobic interactions detected in unfolded apoflavodoxin by paramagnetic relaxation enhancement

Sanne M. Nabuurs · Bregje J. de Kort · Adrie H. Westphal · Carlo P. M. van Mierlo

Received: 10 July 2009 / Revised: 30 September 2009 / Accepted: 9 October 2009 / Published online: 6 November 2009

Abstract Transient structures in unfolded proteins are important in elucidating the molecular details of initiation of protein folding. Recently, native and non-native secondary structure have been discovered in unfolded *A. vinelandii* flavodoxin. These structured elements transiently interact and subsequently form the ordered core of an off-pathway folding intermediate, which is extensively formed during folding of this α–β parallel protein. Here, site-directed spin-labelling and paramagnetic relaxation enhancement are used to investigate long-range interactions in unfolded apoflavodoxin. For this purpose, glutamine-48, which resides in a non-native α-helix of unfolded apoflavodoxin, is replaced by cysteine. This replacement enables covalent attachment of nitroxide spin-labels MTSL and CMTSL. Substitution of Gln-48 by Cys-48 destabilises native apoflavodoxin and reduces flexibility of the ordered regions in unfolded apoflavodoxin in 3.4 M GuHCl, because of increased hydrophobic interactions in the unfolded protein. Here, we report that in the study of the conformational and dynamic properties of unfolded proteins interpretation of spin-label data can be complicated. The covalently attached spin-label to Cys-48 (or Cys-69 of wild-type apoflavodoxin) perturbs the unfolded protein, because hydrophobic interactions occur between the label and hydrophobic patches of unfolded apoflavodoxin. Concomitant hydrophobic free energy changes of the unfolded protein (and possibly of the off-pathway intermediate) reduce the stability of native spin-labelled protein against unfolding. In addition, attachment of MTSL or CMTSL to Cys-48 induces the presence of distinct states in unfolded apoflavodoxin. Despite these difficulties, the spin-label data obtained here show that non-native contacts exist between transiently ordered structured elements in unfolded apoflavodoxin.

Keywords Unfolded protein · Flavodoxin · α–β Parallel protein · Paramagnetic relaxation enhancement · MTSL · CMTSL

The more you see: spectroscopy in molecular biophysics.

S. M. Nabuurs · B. J. de Kort · A. H. Westphal · C. P. M. van Mierlo (✉)
Laboratory of Biochemistry, Wageningen University, Dreijenlaan 3, 6703 HA Wageningen, The Netherlands
e-mail: carlo.vanmierlo@wur.nl

Present Address:
S. M. Nabuurs
Department of Physiology, Radboud University Nijmegen Medical Center, Nijmegen, The Netherlands

Present Address:
B. J. de Kort
Department of Biomedical Analysis, Utrecht University, Utrecht, The Netherlands

Introduction

Understanding the molecular mechanisms of protein folding is one of the fundamental challenges of structural biology. Proteins initially fold from disordered unfolded states. Transient structures in unfolded proteins are important in elucidation of the molecular details of initiation of protein folding. Early observations of residual structure in unfolded proteins prompted the suggestion that native-like structure is present in the denatured state (Gillespie and Shortle 1997; Yi et al. 2000; Lietzow et al. 2002) and that this residual structure biases the subsequent conformational search toward the native conformation (Yi et al. 2000; Daggett and Fersht 2003). However, evidence

of non-native structure has been found in the unfolded states of few proteins (Kristjansdottir et al. 2005; Platt et al. 2005; Reed et al. 2006; Marsh et al. 2007).

Recently, non-native secondary structure and non-native hydrophobic interactions have been observed in the unfolded state of a 179-residue flavodoxin from *Azotobacter vinelandii* (Nabuurs et al. 2008), which is the protein of interest in the study presented here. Remarkably, structure formation in unfolded flavodoxin does not direct folding to the native state, but instead causes formation of a misfolded off-pathway intermediate (Nabuurs et al. 2009a).

Flavodoxins are monomeric proteins involved in electron transport and contain a non-covalently bound flavin mononucleotide (FMN) cofactor. The proteins consist of a single structural domain and adopt the flavodoxin-like or α–β parallel topology (Fig. 1), which is widely prevalent in nature.

Both denaturant-induced equilibrium and kinetic (un)folding of flavodoxin and apoflavodoxin (i.e., flavodoxin without FMN) have been characterized using guanidine hydrochloride (GuHCl) as denaturant (van Mierlo et al. 1998; van Mierlo and Steensma 2000; Bollen et al. 2004, 2005, 2006; Bollen and van Mierlo 2005). The folding data show that apoflavodoxin autonomously folds to its native state, which is structurally identical with that of flavodoxin except that residues in the flavin-binding region of the apo protein have considerable dynamics (Steensma et al. 1998; Steensma and van Mierlo 1998). Binding of FMN to native apoflavodoxin is the last step in flavodoxin folding.

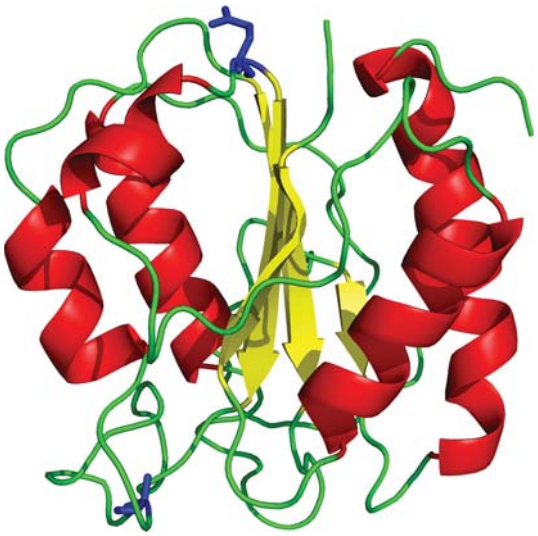

Fig. 1 Schematic diagram of native C69A flavodoxin from *A. vinelandii* (pdb ID 1YOB (Alagaratnam et al. 2005)). The protein contains a parallel β-sheet surrounded by α-helices at either side of the sheet. Residues Ala-69 and Gln-48 are shown in *ball-and-stick* representation (*coloured blue*). The FMN cofactor is not shown

Apoflavodoxin kinetic folding involves an energy landscape with two folding intermediates and is described by: $I_{off} \leftrightarrow$ unfolded apoflavodoxin $\leftrightarrow I_{on} \leftrightarrow$ native apoflavodoxin (Bollen et al. 2004). Intermediate I_{on} lies on the productive route from unfolded to native protein, is highly unstable and is, therefore, not observed during denaturant-induced equilibrium unfolding of apoflavodoxin. Consequently, GuHCl-induced equilibrium unfolding of apoflavodoxin is described by: $I_{off} \leftrightarrow$ unfolded apoflavodoxin $\leftrightarrow$ native apoflavodoxin (Bollen et al. 2004). Approximately 90% of folding molecules fold via molten globule-like off-pathway intermediate I_{off}, which is a relatively stable species that needs to unfold to produce native protein and thus acts as a trap (Bollen et al. 2004). Elevated protein concentrations (van Mierlo et al. 2000) and molecular crowding (Engel et al. 2008) cause severe aggregation of this species. The formation of an off-pathway species is typical for proteins with a flavodoxin-like topology (Bollen and van Mierlo 2005). An off-pathway intermediate is experimentally observed for all other α–β parallel proteins of which the kinetic folding has been investigated, i.e., apoflavodoxin from *Anabaena* (Fernandez-Recio et al. 2001), CheY (Kathuria et al. 2008), cutinase (Otzen et al. 2007), and UMP/CMP kinase (Lorenz and Reinstein 2008).

To better understand why the off-pathway intermediate is formed during flavodoxin folding, GuHCl-unfolded apoflavodoxin has been characterized at the residue-level using heteronuclear NMR spectroscopy (Nabuurs et al. 2008, 2009a). Secondary shifts analysis and investigation of ^{1}H–^{15}N relaxation rates reveal four structured elements that transiently exist in unfolded apoflavodoxin. These transiently ordered regions have restricted flexibility on the (sub)nanosecond timescale and comprise residues Ala-41–Gly-53, Glu-72–Gly-83, Gln-99–Ala-122, and Thr-160–Gly-176 (Nabuurs et al. 2008). These regions match with regions of large average area buried upon folding (AABUF), which correlates with hydrophobicity (Rose and Roy 1980) and corresponds to sequence-dependent dynamic variations due to hydrophobic interactions in unfolded proteins (Schwarzinger et al. 2002; Le Duff et al. 2006).

Restricted flexibility in unfolded apoflavodoxin is due to transient helix formation and local and non-local hydrophobic interactions (Nabuurs et al. 2008, 2009a). On reducing the denaturant concentration, the four structured elements in unfolded apoflavodoxin transiently interact and subsequently form the ordered core of the molten globule (Nabuurs et al. 2008, 2009a). As a consequence, the molten globule has a totally different topology compared with native apoflavodoxin: it is helical and contains no β-sheet (Nabuurs et al. 2009b). Structure formation within virtually all parts of unfolded apoflavodoxin precedes folding to the

molten globule state. This folding transition is non-cooperative and involves a series of distinct transitions (Nabuurs et al. 2009a). Part of I_{off} remains random coil down to a GuHCl concentration of 1.58 M (i.e., residues Lys-13 to Val-36).

To probe long-range interactions in unfolded apoflavodoxin and to consolidate the findings of non-native interactions that lead to formation of the off-pathway intermediate, in the study presented here use is made of site-directed spin-labelling. Paramagnetic relaxation agents are often used to investigate long-distance interactions in unfolded proteins (Dyson and Wright 2005). Site-specific labelling with thiol-specific nitroxide electron spin-labels, for example MTSL ((1-oxy-,2,2,5,5-tetramethyl-D-pyrroline-3-methyl)-methanethiosulfonate) (Berliner et al. 1982) or CMTSL ((1-oxy-,2,2,5,5-tetramethylpyrroline-3-yl)-carbamidoethyl methanethiosulfonate) (Card et al. 2005) (Fig. 2), enables determination of long-range contacts in unfolded proteins (Mittag and Forman-Kay 2007). MTSL (or CMTSL) can exist in two electronic states, an oxidized paramagnetic state and a reduced diamagnetic state. In the oxidized state an unpaired electron in MTSL (or CMTSL) reduces the intensity of NMR signals of atoms that are within approximately 20 to 25 Å of the spin-label, making it a workable probe of distances in the range from 10 to 20 Å in folded proteins (Gillespie and Shortle 1997). This phenomenon of signal intensity reduction is called paramagnetic relaxation enhancement (PRE). Regions of a polypeptide chain that form tertiary interactions with the spin-labelled region will exhibit strong PRE effects. Conversely, regions that remain distant at all times from the spin-labelled region should exhibit weak PRE effects.

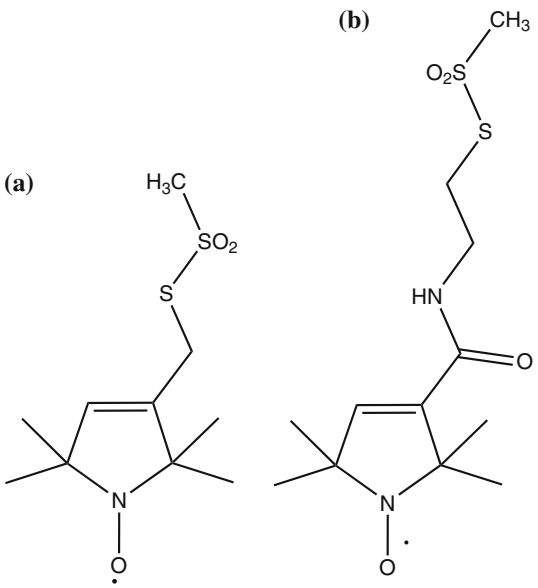

Fig. 2 Schematic representations of the chemical structures of the hydrophobic compounds MTSL (**a**) and CMTSL (**b**). Because of the presence of an amide group in the linker between protein and the proxyl ring in CMTSL this spin-label is more polar than MTSL

Wild-type flavodoxin contains a single cysteine at position 69. This cysteine is poorly accessible to solvent in the holo form of the protein, because of the presence of FMN. However, in apoflavodoxin it is solvent accessible and can be used to attach a spin-label to the protein. Another variant of apoflavodoxin with a single cysteine was made for the purpose of the study presented here. In the latter variant, Gln-48, which resides in the non-native α-helix that is formed in unfolded apoflavodoxin (Nabuurs et al. 2008), is replaced by cysteine. In native apoflavodoxin Gln-48 and Cys-69 are positioned at opposite sites of the protein (Fig. 1).

Here, we show that attachment of a hydrophobic spin-label leads to hydrophobic interactions between the spin-label and various residues of an unfolded protein. Such perturbation of an unfolded protein has not been reported previously, despite the common use of spin-labels to characterise unfolded proteins. Still, even though this perturbation exists, valid information about residual structure in unfolded apoflavodoxin is obtained.

Materials and methods

Sample preparation

Site-directed mutagenesis was used to replace the single cysteine in wild-type *A. vinelandii* (strain ATCC 478) flavodoxin II (i.e., WT flavodoxin) by alanine (i.e., C69A flavodoxin, which is largely similar to WT flavodoxin (Steensma et al. 1996; van Mierlo et al. 1998)). In addition, glutamine at position 48 was replaced by cysteine, resulting in the double mutant C69A-Q48C flavodoxin, hereafter named Q48C flavodoxin.

Uniformly ^{15}N-labelled Q48C and C69A flavodoxins were obtained from transformed *E. coli* cells grown on ^{15}N-labelled algae medium (Silantes, Germany). Uniformly ^{15}N-labelled WT flavodoxin was obtained from transformed *E. coli* cells grown on ^{15}N-labelled minimal medium. All protein variants were purified as described elsewhere (van Mierlo et al. 1998).

Unfolded apoflavodoxin was obtained by denaturing flavodoxin in 6 M GuHCl. Subsequently, FMN was removed via gel filtration in 5 M GuHCl. WT and Q48C protein variants were labelled with MTSL or CMTSL (Toronto Research Chemicals, Toronto, Canada) by adding a 3:1 molar ratio of spin-label to unfolded protein at room temperature. After 2 h, free spin-label was separated from labelled protein by gel filtration. Spin-labelled WT and Q48C apoflavodoxin are referred to as $WT^{(C)MTSL}$ and $Q48C^{(C)MTSL}$ apoflavodoxin, respectively.

All NMR samples contained about 0.3–0.5 mM apoflavodoxin, 10% D_2O, and 2,2-dimethyl-2-silapentane-5-sulfonic acid (DSS) as internal chemical shift reference. To avoid covalent dimerisation of protein molecules that are not spin-labelled, a sufficient amount of DTT was present in samples of WT and Q48C apoflavodoxin.

The buffer used in all experiments was 100 mM potassium pyrophosphate (KPPi), pH 6.0, and refractometry was used to verify GuHCl concentration (Nozaki 1972).

NMR experiments

Gradient enhanced ^1H–^{15}N HSQC spectra were recorded on a Bruker Avance 700 MHz machine. Sample temperature was kept at 25°C. In the ^1H dimension of the ^1H–^{15}N HSQC experiments, 2048 complex data points were acquired, whereas in the indirect ^{15}N dimension 360 complex data points were collected. Spectral widths were 6010 and 1750 Hz in t_2 and t_1, respectively, and the number of scans was 16. All NMR experiments performed with spin-labelled protein in the paramagnetic state were repeated using spin-labelled protein in the diamagnetic state. Diamagnetic protein was obtained by adding 5 µl concentrated stock solution of ascorbic acid to the NMR samples containing paramagnetic protein (the resulting dilution of the NMR sample was less than 1%). This addition resulted in a threefold molar excess of ascorbic acid compared with protein.

Fluorescence spectroscopy

Thermal unfolding of C69A apoflavodoxin, Q48C apoflavodoxin, and $Q48C^{MTSL}$ apoflavodoxin was followed by fluorescence emission. Protein unfolding was achieved by increasing the temperature in a 1.5-ml stirred quartz cuvette (path-length 0.4 cm) from 20 to 70°C at a rate of 0.5°/min. Temperature was measured in the cuvette by using an internal probe. The excitation wavelength used was 280 nm, and fluorescence emission was recorded at 340 nm. Excitation and emission slits were set at 5 nm. In thermal unfolding experiments, protein was in 100 mM KPPi, pH 6.0, and protein concentration ranged between 4 and 6 µM.

Data analysis

NMR data

All NMR data were processed using NMRPipe (Delaglio et al. 1995) and analysed using NMRViewJ (Johnson and Blevins 1994). Paramagnetic relaxation enhancements by nitroxide spin-labels in unfolded apoflavodoxin variants were measured as ratios of maximal cross peak intensities, *I,* between ^1H–^{15}N HSQC spectra of unfolded $WT^{(C)MTSL}$ or $Q48C^{(C)MTSL}$ apoflavodoxin in the paramagnetic and diamagnetic state, respectively:

$$\text{Intensity ratio} = I_{\text{para}}/I_{\text{dia}} \tag{1}$$

Thermally induced equilibrium unfolding data

The change in free energy for thermally induced protein unfolding, $\Delta G(T)$, is described by the modified Gibbs–Helmholtz equation:

$$\Delta G(T) = \Delta H_{\text{m}}(1 - T/T_{\text{m}}) - \Delta C_{\text{p}}[(T_{\text{m}} - T) + T\ln(T/T_{\text{m}})] \tag{2}$$

where ΔH_{m} is the enthalpy change for unfolding measured at T_{m}, T is the absolute temperature, T_{m}, is the temperature at the midpoint of the (un)folding transition, and ΔC_{p} is the difference in heat capacity between the unfolded and folded states (Pace and Laurents 1989). Under the assumption that ΔC_{p} is temperature-independent (Privalov and Khechinashvili 1974; Becktel and Schellman 1987), a two-state mechanism of unfolding can be fitted to individual thermal unfolding curves:

$$Y_{\text{obs}} = (a_{\text{U}} + b_{\text{U}}T) + \frac{((a_{\text{N}} + b_{\text{N}}T) - (a_{\text{U}} + b_{\text{U}}T))}{(1 + \exp(((-\Delta H_{\text{m}}/R)(1/T - 1/T_{\text{m}})) + ((\Delta C_{\text{p}}/R)(((T_{\text{m}}/T) - 1) + \ln(T/T_{\text{m}})))))} \tag{3}$$

where Y_{obs} is the measured fluorescence signal, R is the gas constant, and a and b are the intercepts and slopes, respectively, of the pre-unfolding and post-unfolding baselines.

Results and discussion

Introducing a cysteine at position 48 and subsequent labelling with MTSL both reduce the thermal midpoint of unfolding of apoflavodoxin

Thermal-induced unfolding experiments show that replacement of Gln-48 by Cys-48 destabilizes native apoflavodoxin in 100 mM KPPi at pH 6.0. Fluorescence emission enables monitoring of unfolding of native protein molecules, because both folding intermediate and unfolded apoflavodoxin have comparable fluorescence signals. Using fluorescence emission, the thermal midpoint of unfolding (T_{m}) of Q48C apoflavodoxin is determined to be 40.4 ± 0.2°C, whereas C69A apoflavodoxin has a T_{m} of 48.2 ± 0.1°C (Fig. 3). Attachment of the MTSL spin-label to Cys-48 further reduces T_{m} to 33.0 ± 1.6°C.

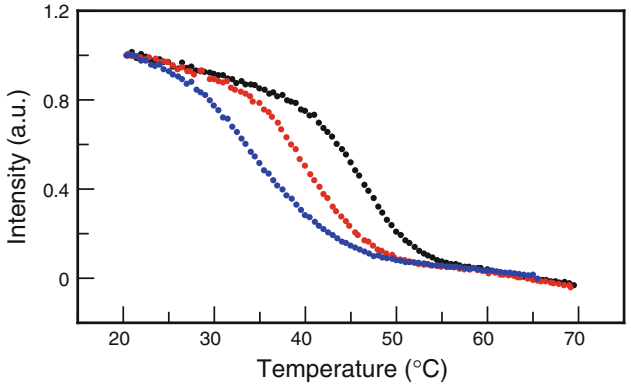

Fig. 3 Thermal unfolding of apoflavodoxin shows that replacement of Gln-48 by Cys-48 and subsequent attachment of an MTSL spin-label to Cys-48 both destabilize the protein against thermal unfolding. Through detection of changes in fluorescence emission at 340 nm thermal unfolding is measured for C69A apoflavodoxin (*black dots*), Q48C apoflavodoxin (*red dots*), and Q48C^{MTSL} apoflavodoxin (*blue dots*). Midpoints of unfolding are 48.2 ± 0.1°C for C69A apoflavodoxin, 40.4 ± 0.2°C for Q48C apoflavodoxin, and 33.0 ± 1.6°C for Q48C^{MTSL} apoflavodoxin

Introducing a cysteine at position 48 changes the dynamic features of unfolded apoflavodoxin

Comparison of chemical shifts of cross peaks in ^{1}H–^{15}N HSQC spectra of Q48C and C69A apoflavodoxin in 3.4 M GuHCl previously showed that replacement of a glutamine by a cysteine at position 48 leads to chemical shift changes in unfolded apoflavodoxin. These chemical shift changes indicate long-range non-native interactions between transiently formed helices in unfolded apoflavodoxin (Nabuurs et al. 2008).

In 3.4 M GuHCl, several cross peak intensities of unfolded Q48C apoflavodoxin are reduced compared with the cross peak intensities of the backbone amides of unfolded C69A apoflavodoxin, because of broadening of cross peaks. This broadening is caused by reduced flexibility of backbone amides. Fig. 4 shows that four distinct regions in unfolded Q48C apoflavodoxin have reduced flexibility of their backbone amides compared with the corresponding amides of unfolded C69A apoflavodoxin. These distinct regions coincide with the four regions with restricted flexibility detected in unfolded C69A apoflavodoxin (Nabuurs et al. 2008), which are highlighted by grey bars in Fig. 4. Consequently, upon replacing Gln-48 by Cys-48 the four regions with restricted flexibility in unfolded apoflavodoxin become even less flexible, probably because of non-native hydrophobic interactions between Cys-48 and the four ordered regions identified.

Unfolded Q48C apoflavodoxin in 6.0 M GuHCl behaves as a random coil; subsequent attachment of MTSL causes the protein to become more ordered

Far-UV CD data and transverse relaxation rates (Nabuurs et al. 2008) show that C69A apoflavodoxin in 6.0 M GuHCl behaves as a random coil. The Q48C variant of apoflavodoxin is also a random coil in 6.0 M GuHCl. This random coil behaviour is concluded because the ^{1}H–^{15}N HSQC spectra of both Q48C and C69A apoflavodoxin at this concentration denaturant are very similar regarding both cross peak positions and cross peak intensities (data not shown).

The ratios between cross peak intensities of reduced Q48C^{MTSL} and Q48C apoflavodoxin, both unfolded in 6.0 M GuHCl, are shown in Fig. 5. The direct sequential neighbours of Cys-48 are either not visible or could not be assigned in the ^{1}H–^{15}N HSQC spectrum of Q48C^{MTSL} apoflavodoxin. In 6.0 M GuHCl, the backbone amides of Ser-40, Ala-41, Glu-42, Ile-51, Leu-52, and Gly-53 of reduced Q48C^{MTSL} apoflavodoxin have reduced intensities compared with the corresponding intensities in the HSQC spectrum of Q48C apoflavodoxin (Fig. 5). Restricted motions of these residues because of interactions with MTSL most likely cause this decrease.

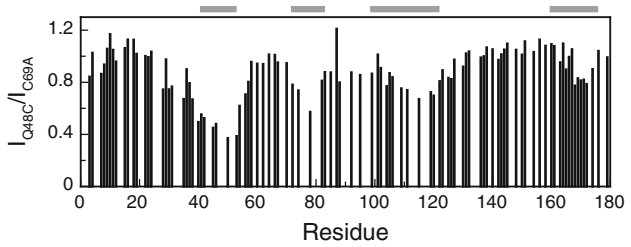

Fig. 4 Upon replacing Gln-48 by Cys-48 the four regions with restricted flexibility in unfolded apoflavodoxin in 3.4 M GuHCl become less flexible. Shown are the ratios between cross peak intensities of backbone amides of unfolded Q48C apoflavodoxin (I_{Q48C}) and unfolded C69A apoflavodoxin (I_{C69A}). The ratio I_{Q48C}/I_{C69A} of residue 179 is set to 1. *Horizontal grey bars* highlight the four regions of unfolded C69A apoflavodoxin with restricted flexibility on the (sub)nanosecond timescale (Nabuurs et al. 2008)

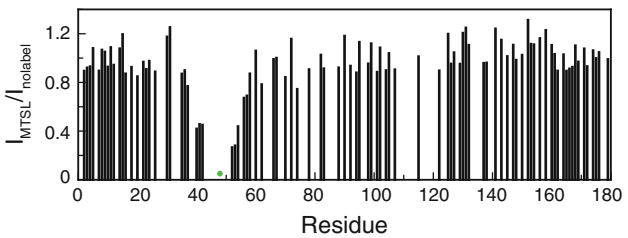

Fig. 5 Attachment of MTSL to unfolded Q48C apoflavodoxin in 6.0 M GuHCl causes the protein to behave in a more ordered fashion than random coil apoflavodoxin. Shown are the ratios between cross peak intensities of backbone amides of unfolded Q48C^{MTSL} apoflavodoxin in the diamagnetic state (I_{MTSL}) and unfolded Q48C apoflavodoxin ($I_{nolabel}$), which are both in 6.0 M GuHCl. The ratio $I_{MTSL}/I_{nolabel}$ of residue 179 is set to 1. The *green dot* indicates the position of the spin-label

In conclusion, attachment of MTSL to unfolded Q48C apoflavodoxin in 6.0 M GuHCl causes the protein to behave in a more ordered fashion than random coil apoflavodoxin.

Use of PRE experiments

Magnetic interaction between an unpaired electron in a paramagnetic nitroxide spin-label and a nearby proton causes broadening of the corresponding ^{1}H NMR signal because of the increased transverse relaxation rate of the proton involved (Gillespie and Shortle 1997). This relaxation rate has an r^{-6}-dependence on electron–proton distance and thus enables detection of long-range interactions in proteins. Consequently, ratios of cross peak intensities (I_{para}/I_{dia}) extracted from two redox state-dependent ^{1}H–^{15}N HSQC spectra of the spin-labelled protein enable estimation of distances between the spin-label and affected protons in the protein (Teilum et al. 2002). Because of the ubiquitous backbone fluctuations in unfolded apoflavodoxin (Nabuurs et al. 2008), no attempt is made to extract quantitative distances from the data. Rather, a trend in PRE as a function of primary structure can be observed, as shown in the following discussion.

PRE shows that WT^{MTSL} apoflavodoxin in 6.0 M GuHCl does not behave as a random coil, because of hydrophobic interactions between MTSL and unfolded protein

^{1}H–^{15}N HSQC spectra were acquired of MTSL-labelled WT apoflavodoxin and Q48C apoflavodoxin both unfolded in 6.0 M GuHCl, with the spin-label either in the paramagnetic or the diamagnetic state. Subsequently, the ratios of the intensities of cross peak maxima (I_{para}/I_{dia}) of backbone amides were determined. Fig. 6 shows these ratios and demonstrates that for both protein variants resonances of residues that are sequential neighbours of the cysteine to which a nitroxide radical is attached are broadened beyond detection. In addition, for WT^{MTSL} apoflavodoxin the nitroxide radical also reduces the backbone amide cross peak intensities of residues Ser-40–Leu-62. PRE data of WT^{MTSL} apoflavodoxin thus indicate that Gln-48 is in the vicinity of the spin-label that is attached to Cys-69. Our observations show that in 6.0 M GuHCl WT^{MTSL} apoflavodoxin does not behave as a random coil.

In contrast with the above observation, PRE data of Q48C^{MTSL} apoflavodoxin (Fig. 6b) show no evidence of an interaction between Cys-48 and Ala-69. Note however, as discussed in a previous section, that attachment of MTSL to unfolded Q48C apoflavodoxin in 6.0 M GuHCl causes the protein to behave more ordered than random coil apoflavodoxin. The nitroxide radical of MTSL attached to

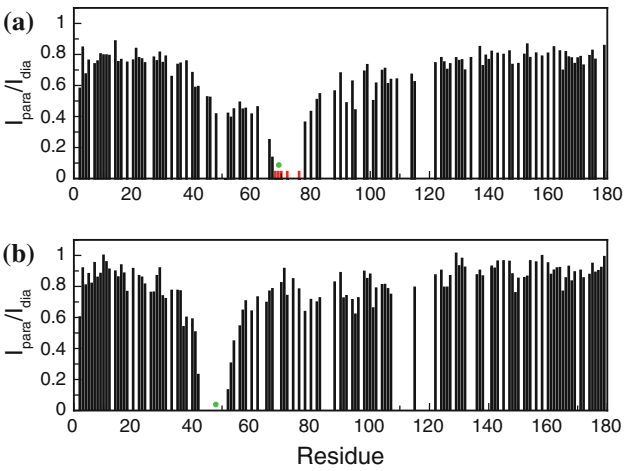

Fig. 6 PRE of amide protons of WT^{MTSL} apoflavodoxin and Q48C^{MTSL} apoflavodoxin, which are both unfolded in 6.0 M GuHCl. ^{1}H–^{15}N HSQC spectra of both protein variants with the spin-label either in the paramagnetic or diamagnetic state were recorded at 25°C. Subsequently, the ratio of the intensities of cross peak maxima (I_{para}/I_{dia}) of backbone amides was determined. Shown are I_{para}/I_{dia} of **a** WT^{MTSL} apoflavodoxin and **b** Q48C^{MTSL} apoflavodoxin. *Green dots* highlight the positions of the spin-label. *Red bars* in (**a**) highlight residues for which no cross peaks are visible in the HSQC spectrum of the protein with paramagnetic spin-label, but for which cross peaks are observed when the spin-label is diamagnetic

Cys-48 does not broaden resonances of residues in the vicinity of Ala-69 (the cross peak of the backbone amide of Ala-69 suffers from severe overlap and is thus not assigned). The interaction between the MTSL spin-label attached to Cys-69 and region Ser-40–Leu-62 of unfolded apoflavodoxin in 6.0 M GuHCl is thus due to hydrophobic interactions of the label with residues in this region. Similar hydrophobic interactions with MTSL spin-label were also observed in dimerization studies of ARNT PAS-B (Card et al. 2005).

In both WT^{CMTSL} and Q48C^{CMTSL} apoflavodoxin unfolded in 3.4 M GuHCl the spin-label interacts with four transiently structured regions

To reduce hydrophobic interactions in unfolded apoflavodoxin due to MTSL, another spin-label, i.e., CMTSL (Card et al. 2005), which is more hydrophilic than MTSL, was chosen as paramagnetic relaxation agent. Compared with MTSL, CMTSL contains an additional amide group in the linker between protein and the proxyl ring (Fig. 2), thereby introducing a degree of polarity into an otherwise hydrophobic compound.

Figure 7a and b show the ratios of the intensities of HSQC cross peak maxima (I_{para}/I_{dia}) of backbone amides of the paramagnetic and diamagnetic states of WT^{CMTSL} apoflavodoxin and Q48C^{CMTSL} apoflavodoxin, respectively, which are both unfolded in 6.0 M GuHCl. The

pattern of interactions of the CMTSL spin-label in both unfolded proteins is similar to the pattern of interactions observed using MTSL as spin-label. Consequently, also with CMTSL attached to unfolded apoflavodoxin in 6.0 M GuHCl, hydrophobic interactions exist between the spin-label at position 69 and the hydrophobic region comprising residues 40–60 of unfolded apoflavodoxin.

In Fig. 7c and d PRE data of WT^{CMTSL} and $Q48C^{CMTSL}$ apoflavodoxin in 3.4 M GuHCl are shown. In both WT^{CMTSL} and $Q48C^{CMTSL}$ apoflavodoxin the CMTSL spin-label interacts with various regions of the unfolded protein. In particular, interactions are observed between the spin-label and the four transiently structured regions in unfolded apoflavodoxin in 3.4 M GuHCl, strengthening our previous findings (Nabuurs et al. 2008) that non-native

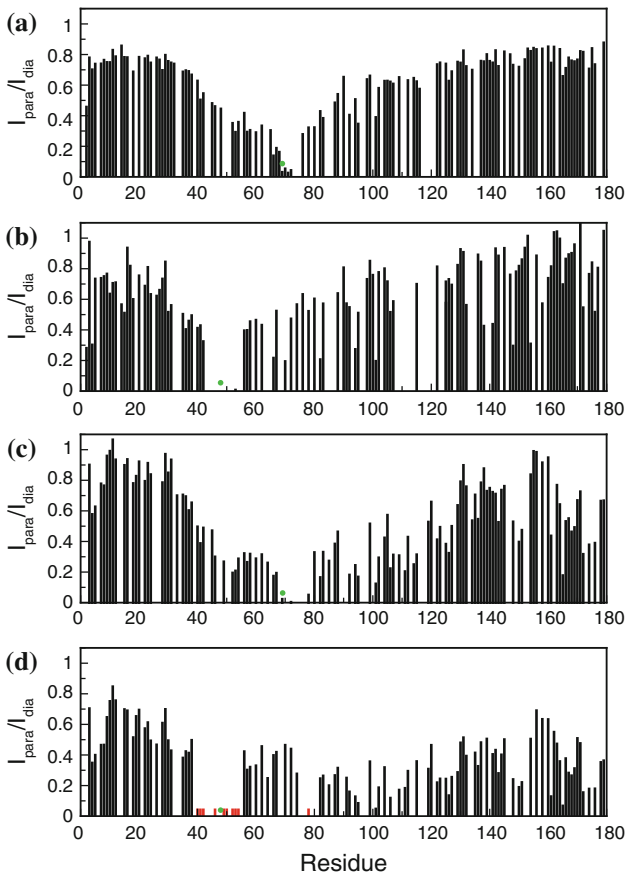

Fig. 7 PRE of amide protons of WT^{CMTSL} and $Q48C^{CMTSL}$ apoflavodoxin unfolded in GuHCl at 25°C. The ratio of the intensities of HSQC cross peak maxima (I_{para}/I_{dia}) of backbone amides was determined as described in the legend of Fig. 6. Shown are I_{para}/I_{dia} of **a** WT^{MTSL} and **b** $Q48C^{MTSL}$ apoflavodoxin, both in 6.0 M GuHCl, and I_{para}/I_{dia} of **c** WT^{MTSL} and **d** $Q48C^{MTSL}$, both in 3.4 M GuHCl. Green dots highlight the positions of the CMTSL spin-label. Residues Ser-40, Ala-41, Glu-42, Gln-46, Phe-49, Leu-50, Leu-52, Gly-53, Thr-54, and Leu-78 of $Q48C^{CMTSL}$ apoflavodoxin in 3.4 M GuHCl each give rise to two backbone amide cross peaks (a few examples are shown in Fig. 8) and are indicated with *red bars* in (**d**)

contacts do, indeed, exist between transiently ordered structured elements in unfolded apoflavodoxin.

In $Q48C^{CMTSL}$ apoflavodoxin unfolded in 3.4 M GuHCl, the spin-label interacts with residues spread over the entire sequence of the protein. Residues 40 to 54 and Leu-78 stand out, as the corresponding backbone amide resonances are broadened beyond detection in the paramagnetic state of the unfolded protein. These residues will be discussed in the next section. In addition, resonances of residues 82 to 129 are more severely broadened than the resonances of most of the residues of unfolded $Q48C^{CMTSL}$ apoflavodoxin.

The attached spin-label induces the presence of two distinct states in unfolded apoflavodoxin

We notice that in the HSQC spectrum of reduced $Q48C^{MTSL}$ and $Q48C^{CMTSL}$ apoflavodoxin in 3.4 M GuHCl multiple cross peaks are observed for several backbone amides. We focus here on $Q48C^{CMTSL}$ apoflavodoxin for which two cross peaks are observed for each individual backbone amide of residues Ser-40, Ala-41, Glu-42, Gln-46, Phe-49, Leu-50, Leu-52, Gly-53, Thr-54, and Leu-78. In Fig. 8 examples of this cross peak doubling are shown. For each doubled cross peak it is observed that upon bringing the spin-label into the paramagnetic state one of these two cross peaks broadens beyond detection (this disappearing cross peak is used to calculate I_{para}/I_{dia} of the corresponding residues in Fig. 7c,d). Doubling of the cross peaks of the residues mentioned is not because of the presence of non-labelled protein molecules. In the latter case, additional cross peaks would appear at different positions in the HSQC spectrum, as the HSQC spectrum of Q48C apoflavodoxin in 3.4 M GuHCl shows (Fig. 8).

A plausible explanation of the observed doubling of cross peaks is that the attached spin-label induces the presence of two distinct states in unfolded apoflavodoxin. In one of these states the spin-label is in the proximity of the above-mentioned residues whereas in the other state it is not. Both folding states are in slow exchange with one another on the NMR chemical shift time scale, because two separate, sharp cross peaks are observed per backbone amide of the residues discussed.

Leu-78 is the only residue that is not sequentially close to the CMTSL-label at position 48, but nevertheless gives rise to two backbone amide cross peaks. Indeed, chemical shift deviations upon replacing residue 48 show that interactions between Cys-48 and Leu-78 must exist in unfolded apoflavodoxin (Nabuurs et al. 2008). Residual structure that is neither an α-helix nor a β-sheet is found in the region Glu-72–Gly-83 of unfolded apoflavodoxin (Nabuurs et al. 2008). These observations are further support for the existence of persistent hydrophobic interactions between Leu-78 and the CMTSL spin-label in one of the

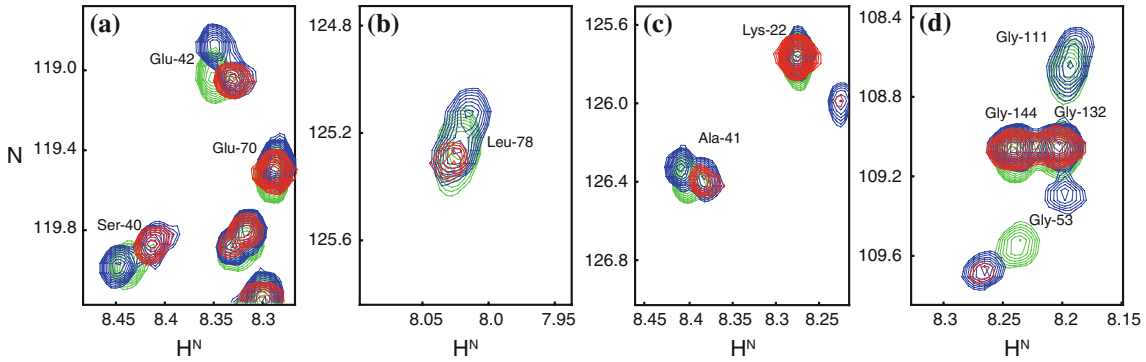

Fig. 8 A backbone amide that is in close vicinity to the CMTSL spin-label of Q48C^{CMTSL} apoflavodoxin in 3.4 M GuHCl can give rise to two cross peaks in the corresponding ^{1}H–^{15}N HSQC spectrum. *Blue contour levels* highlight cross peaks arising from diamagnetic Q48C^{CMTSL} apoflavodoxin, *red contour levels* highlight cross peaks arising from paramagnetic Q48C^{CMTSL} apoflavodoxin, and *green contour levels* highlight cross peaks arising from Q48C apoflavodoxin with no spin-label attached to it. A set of two cross peaks is shown for **a** Ser-40 and Glu-42, **b** Leu-78, **c** Ala-41 and for **d** Gly-53

two distinct states within unfolded Q48C^{CMTSL} apoflavodoxin. The tertiary interaction between residues 48 and 78 in unfolded apoflavodoxin, as revealed by PRE experiments, must be non-native. The latter is concluded because complete disappearance of the backbone amide cross peak of Leu-78 implies that the distance between residues 48 and 78 must be much shorter than the 17.28 Å distance between the corresponding Cα atoms in native flavodoxin (calculated using the X-ray structure of *A. vinelandii* flavodoxin (Alagaratnam et al. 2005)).

Introducing cysteine residues in (unfolded) proteins to enable labelling with probes is used frequently (Fanucci and Cafiso 2006; Clore et al. 2007). To detect long-range interactions within (natively) unfolded proteins, for example apomyoglobin (Lietzow et al. 2002), α-synuclein (Bertoncini et al. 2005), ACBP (Teilum et al. 2002), and N-PGK (Cliff et al. 2009), MTSL is widely used as a nitroxide spin-label. However, the results presented here show that in an unfolded protein covalent attachment of a spin-label to cysteine can introduce hydrophobic interactions between the hydrophobic spin-label and various amino acid residues. These interactions alter the hydrophobic free energy (Baldwin 2005) of the unfolded state (and possibly of the off-pathway intermediate) and, as a consequence, the free energy difference between native apoflavodoxin and non-native protein molecules diminishes. Indeed, covalent attachment of a MTSL-label can alter the stability of the protein involved, as is shown here for native apoflavodoxin and as is reported for ACBP variants (Teilum et al. 2002). Remarkably, in contrast with unfolded apoflavodoxin, no hydrophobic interactions, either short-range or long-range, with the MTSL-label have been reported for the unfolded proteins mentioned. Neither has doubling of cross peaks of these spin-labelled unfolded proteins been reported.

Native apoflavodoxin is an α–β parallel protein and contains in its core many hydrophobic residues that are shielded from the solvent. It is possible that in unfolded protein these residues are susceptible to hydrophobic interactions with the hydrophobic nitroxide spin-labels used. These interactions can give rise to the existence of distinct states in the unfolded protein, as this work shows. Despite the difficulties mentioned, the spin-label data obtained here show that non-native contacts exist between transiently ordered structured elements in unfolded apoflavodoxin.

Acknowledgments The Netherlands Organization for Scientific Research supported this work. NMR spectra were recorded at the Utrecht Facility for High-Resolution NMR, The Netherlands.

References

Alagaratnam S, van Pouderoyen G, Pijning T, Dijkstra BW, Cavazzini D, Rossi GL, Van Dongen WM, van Mierlo CP, van Berkel WJ, Canters GW (2005) A crystallographic study of Cys69Ala flavodoxin II from *Azotobacter vinelandii*: structural determinants of redox potential. Protein Sci 14:2284–2295

Baldwin RL (2005) Weak interactions in protein folding: hydrophobic free energy, van der Waals interactions, peptide hydrogen bonds, and peptide solvation. In: Buchner J, Kiefhaber T (eds) Protein folding handbook, vol 1. Wiley-VCH, Weinheim, pp 127–162

Becktel WJ, Schellman JA (1987) Protein stability curves. Biopolymers 26:1859–1877

Berliner LJ, Grunwald J, Hankovszky HO, Hideg K (1982) A novel reversible thiol-specific spin label: papain active site labeling and inhibition. Anal Biochem 119:450–455

Bertoncini CW, Jung YS, Fernandez CO, Hoyer W, Griesinger C, Jovin TM, Zweckstetter M (2005) Release of long-range tertiary interactions potentiates aggregation of natively unstructured alpha-synuclein. Proc Natl Acad Sci U S A 102:1430–1435

Bollen YJ, van Mierlo CP (2005) Protein topology affects the appearance of intermediates during the folding of proteins with a flavodoxin-like fold. Biophys Chem 114:181–189

Bollen YJ, Sanchez IE, van Mierlo CP (2004) Formation of on- and off-pathway intermediates in the folding kinetics of *Azotobacter vinelandii* apoflavodoxin. Biochemistry 43:10475–10489

Bollen YJ, Nabuurs SM, van Berkel WJ, van Mierlo CP (2005) Last in, first out: the role of cofactor binding in flavodoxin folding. J Biol Chem 280:7836–7844

Bollen YJ, Kamphuis MB, van Mierlo CP (2006) The folding energy landscape of apoflavodoxin is rugged: hydrogen exchange reveals nonproductive misfolded intermediates. Proc Natl Acad Sci U S A 103:4095–4100

Card PB, Erbel PJ, Gardner KH (2005) Structural basis of ARNT PAS-B dimerization: use of a common beta-sheet interface for hetero- and homodimerization. J Mol Biol 353:664–677

Cliff MJ, Craven CJ, Marston JP, Hounslow AM, Clarke AR, Waltho JP (2009) The denatured state of N-PGK is compact and predominantly disordered. J Mol Biol 385:266–277

Clore GM, Tang C, Iwahara J (2007) Elucidating transient macromolecular interactions using paramagnetic relaxation enhancement. Curr Opin Struct Biol 17:603–616

Daggett V, Fersht A (2003) The present view of the mechanism of protein folding. Nat Rev Mol Cell Biol 4:497–502

Delaglio F, Grzesiek S, Vuister GW, Zhu G, Pfeifer J, Bax A (1995) NMRPipe–a multidimensional spectral processing system based on unix pipes. J Biomol NMR 6:277–293

Dyson HJ, Wright PE (2005) Elucidation of the protein folding landscape by NMR. Methods Enzymol 394:299–321

Engel R, Westphal AH, Huberts DH, Nabuurs SM, Lindhoud S, Visser AJ, van Mierlo CP (2008) Macromolecular crowding compacts unfolded apoflavodoxin and causes severe aggregation of the off-pathway intermediate during apoflavodoxin folding. J Biol Chem 283:27383–27394

Fanucci GE, Cafiso DS (2006) Recent advances and applications of site-directed spin labeling. Curr Opin Struct Biol 16:644–653

Fernandez-Recio J, Genzor CG, Sancho J (2001) Apoflavodoxin folding mechanism: an alpha/beta protein with an essentially off-pathway intermediate. Biochemistry 40:15234–15245

Gillespie JR, Shortle D (1997) Characterization of long-range structure in the denatured state of staphylococcal nuclease.I. Paramagnetic relaxation enhancement by nitroxide spin labels. J Mol Biol 268:158–169

Johnson BA, Blevins RA (1994) NMR view–a computer-program for the visualization and analysis of NMR data. J Biomol NMR 4:603–614

Kathuria SV, Day IJ, Wallace LA, Matthews CR (2008) Kinetic traps in the folding of beta alpha-repeat proteins: CheY initially misfolds before accessing the native conformation. J Mol Biol 382:467–484

Kristjansdottir S, Lindorff-Larsen K, Fieber W, Dobson CM, Vendruscolo M, Poulsen FM (2005) Formation of native and non-native interactions in ensembles of denatured ACBP molecules from paramagnetic relaxation enhancement studies. J Mol Biol 347:1053–1062

Le Duff CS, Whittaker SBM, Radford SE, Moore GR (2006) Characterisation of the conformational properties of urea-unfolded Im7: implications for the early stages of protein folding. J Mol Biol 364:824–835

Lietzow MA, Jamin M, Jane Dyson HJ, Wright PE (2002) Mapping long-range contacts in a highly unfolded protein. J Mol Biol 322:655–662

Lorenz T, Reinstein J (2008) The influence of proline isomerization and off-pathway intermediates on the folding mechanism of eukaryotic UMP/CMP Kinase. J Mol Biol 381:443–455

Marsh JA, Neale C, Jack FE, Choy WY, Lee AY, Crowhurst KA, Forman-Kay JD (2007) Improved structural characterizations of the drkN SH3 domain unfolded state suggest a compact ensemble with native-like and non-native structure. J Mol Biol 367:1494–1510

Mittag T, Forman-Kay JD (2007) Atomic-level characterization of disordered protein ensembles. Curr Opin Struct Biol 17:3–14

Nabuurs SM, Westphal AH, van Mierlo CP (2008) Extensive formation of off-pathway species during folding of an alpha-beta parallel protein is due to docking of (non)native structure elements in unfolded molecules. J Am Chem Soc 130:16914–16920

Nabuurs SM, Westphal AH, van Mierlo CPM (2009a) Noncooperative formation of the off-pathway molten globule during folding of the α–β parallel protein apoflavodoxin. J Am Chem Soc 131:2739–2746

Nabuurs SM, Westphal AH, aan den Toorn M, Lindhoud S, van Mierlo CP (2009b) Topological switching between an alpha-beta parallel protein and a remarkably helical molten globule. J Am Chem Soc 131:8290–8295

Nozaki Y (1972) The preparation of guanidine hydrochloride. In: Hirs CHW, Timasheff SN (eds) Methods in enzymology, vol 26. Academic Press, New York, pp 43–50

Otzen DE, Giehm L, Baptista RP, Kristensen SR, Melo EP, Pedersen S (2007) Aggregation as the basis for complex behaviour of cutinase in different denaturants. Biochim Biophys Acta 1774:323–333

Pace CN, Laurents DV (1989) A new method for determining the heat capacity change for protein folding. Biochemistry 28:2520–2525

Platt GW, McParland VJ, Kalverda AP, Homans SW, Radford SE (2005) Dynamics in the unfolded state of beta2-microglobulin studied by NMR. J Mol Biol 346:279–294

Privalov PL, Khechinashvili NN (1974) A thermodynamic approach to the problem of stabilization of globular protein structure: a calorimetric study. J Mol Biol 86:665–684

Reed MA, Jelinska C, Syson K, Cliff MJ, Splevins A, Alizadeh T, Hounslow AM, Staniforth RA, Clarke AR, Craven CJ, Waltho JP (2006) The denatured state under native conditions: a non-native-like collapsed state of N-PGK. J Mol Biol 357:365–372

Rose GD, Roy S (1980) Hydrophobic basis of packing in globular-proteins. Proc Natl Acad Sci USA 77:4643–4647

Schwarzinger S, Wright PE, Dyson HJ (2002) Molecular hinges in protein folding: The urea-denatured state of apomyoglobin. Biochemistry 41:12681–12686

Steensma E, van Mierlo CP (1998) Structural characterisation of apoflavodoxin shows that the location of the stable nucleus differs among proteins with a flavodoxin-like topology. J Mol Biol 282:653–666

Steensma E, Heering HA, Hagen WR, Van Mierlo CP (1996) Redox properties of wild-type, Cys69Ala, and Cys69Ser *Azotobacter vinelandii* flavodoxin II as measured by cyclic voltammetry and EPR spectroscopy. Eur J Biochem 235:167–172

Steensma E, Nijman MJ, Bollen YJ, de Jager PA, van den Berg WA, van Dongen WM, van Mierlo CP (1998) Apparent local stability of the secondary structure of *Azotobacter vinelandii* holoflavodoxin II as probed by hydrogen exchange: implications for redox potential regulation and flavodoxin folding. Protein Sci 7:306–317

Teilum K, Kragelund BB, Poulsen FM (2002) Transient structure formation in unfolded acyl-coenzyme A-binding protein observed by site-directed spin labelling. J Mol Biol 324:349–357

van Mierlo CP, Steensma E (2000) Protein folding and stability investigated by fluorescence, circular dichroism (CD), and nuclear magnetic resonance (NMR) spectroscopy: the flavodoxin story. J Biotechnol 79:281–298

van Mierlo CP, van Dongen WM, Vergeldt F, van Berkel WJ, Steensma E (1998) The equilibrium unfolding of *Azotobacter*

vinelandii apoflavodoxin II occurs via a relatively stable folding intermediate. Protein Sci 7:2331–2344

van Mierlo CP, van den Oever JM, Steensma E (2000) Apoflavodoxin (un)folding followed at the residue level by NMR. Protein Sci 9:145–157

Yi Q, Scalley-Kim ML, Alm EJ, Baker D (2000) NMR characterization of residual structure in the denatured state of protein L. J Mol Biol 299:1341–1351